# Energy Extraction and Quasinormal Modes of Black Hole Binaries: An analytical and numerical study


Lucas Timotheo Sanches

Advisor: Prof. Dr. Maurício Richartz


05/31/2023


Physics@UFABC

# Presentation Outline

1) The relevance of binary systems
2) Modeling binary systems
3) The Kerr Penrose Process
4) The MP Penrose Process
5) The CMMR Penrose Process
6) Non-Stationary Penrose Process
7) Simulating Wave Scattering on GW150914
8) The Asymptotic Iteration Method and QuasinormalModes.jl
9) Conclusions and perspectives

# The Relevance Of Binary Systems

Accretion Disk Formation

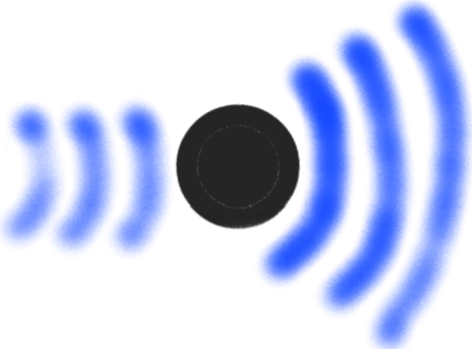

Superradiance

Hawking Radiation

The astrophysical Kerr Black Hole is a two-parameter vacuum solution of EFEs.

Even though they are mathematically very simple, they have very rich interactions with their surroundings

How can we extend these concepts to black hole binaries?

# Modeling Binary Systems

| Static BBH Model | Exact BBH Model | Analitic BBH Model |
| --- | --- | --- |
| Two back holes that do not move with respec to the static observer at infinity. | An exact vacuum solution of Einstein's Field Equations. | The entire spacetime metric is analytically known at all points in space and time. |

| Dynamic BBH Model | Approximate BBH Model | Numeric BBH Model |
| --- | --- | --- |
| Two back holes that move with respect to the static observer at infinity. | Non-exact solution of Einstein's Field Equations. No exotic matter. | Obtained at a hypersurface by numerically solving the ADM constraint equations. |

# The Kerr Penrose Process

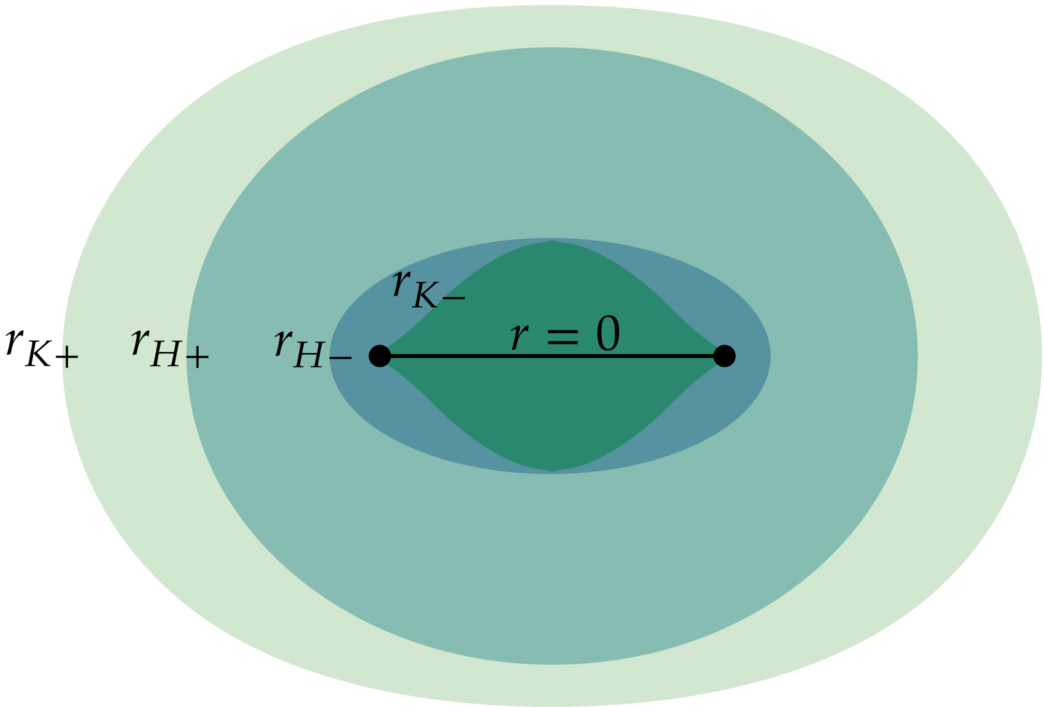


The Kerr spacetime possesses a global time-like Killing vector field.

The outer Killing horizon is located outside the outer event horizon.

The Region between the Killing horizon and outer horizon is known as the Ergosphere

# The Kerr Penrose Process

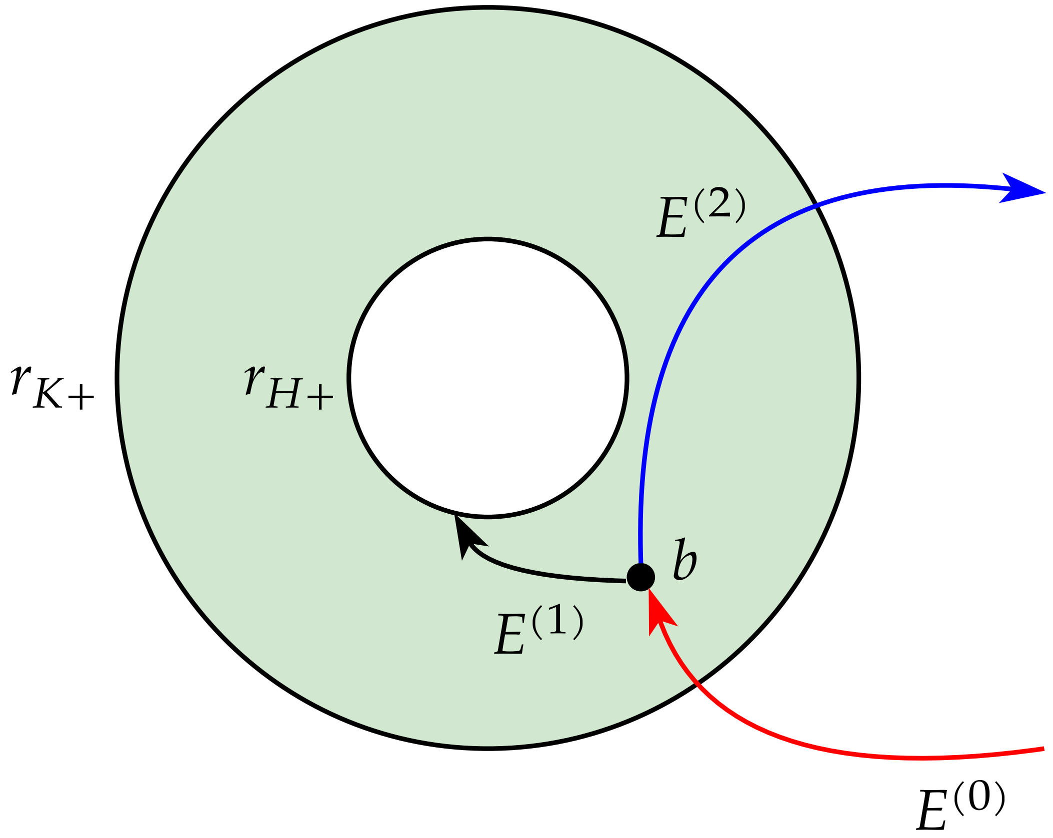


In the ergosphere, a particle may have negative energy according to the static observer at infinity.

One can engineer a particle decay process in such a way that particles leaving the system are more energetic than those entering the system.

In the Kerr metric, this excess energy comes from the black hole's rotation.

# The MP Penrose Process

The Majumdar - Papapetrou solution (MP) describes two extremally charged black holes in static equilibrium, thanks to their charge:

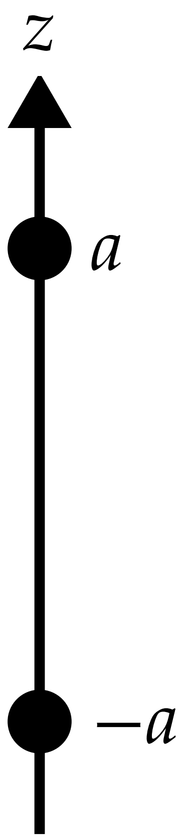


$$ds^2 = -\frac{dt^2}{U(\rho,z)^2} + U(\rho,z)^2\left[d\rho^2 + \rho^2 d\phi^2 + dz^2\right]$$

$$A_\mu = 1 + \frac{M_1}{\sqrt{\rho^2+(z+a)^2}} + \frac{M_2}{\sqrt{\rho^2+(z-a)^2}}$$

$$A_\mu = \left(1 - \frac{1}{U(\rho,z)}\right)\delta_{\mu t}$$

# The MP Penrose Process

A charged particle, moving through this binary has energy given by

$$E = \mu\left(1 - \frac{1}{U}\right) + \sqrt{\frac{L^2}{\rho^2 U^4} + \frac{1}{U^2} + \dot{\rho}^2 + \dot{z}^2}$$

At a fixed position, the minimum possible energy is associated with particles at rest, thus

$$E_{\min} = \mu\left(1 - \frac{1}{U}\right) + \frac{1}{U}$$

The minimum energy will be negative if

$$\mu < 0$$

$$\frac{1}{\sqrt{\bar{\rho}^2 + (\bar{z}+1)^2}} + \frac{M_R}{\sqrt{\bar{\rho}^2 + (\bar{z}-1)^2}} > -\frac{1+M_R}{\bar{\mu}}$$

Where

$$M_R = M_2/M_1 \quad M_T = M_1 + M_2$$

$$\bar{\rho} = \rho/a \quad \bar{z} = z/a \quad \bar{\mu} = \mu M_T/a$$

# The MP Penrose Process

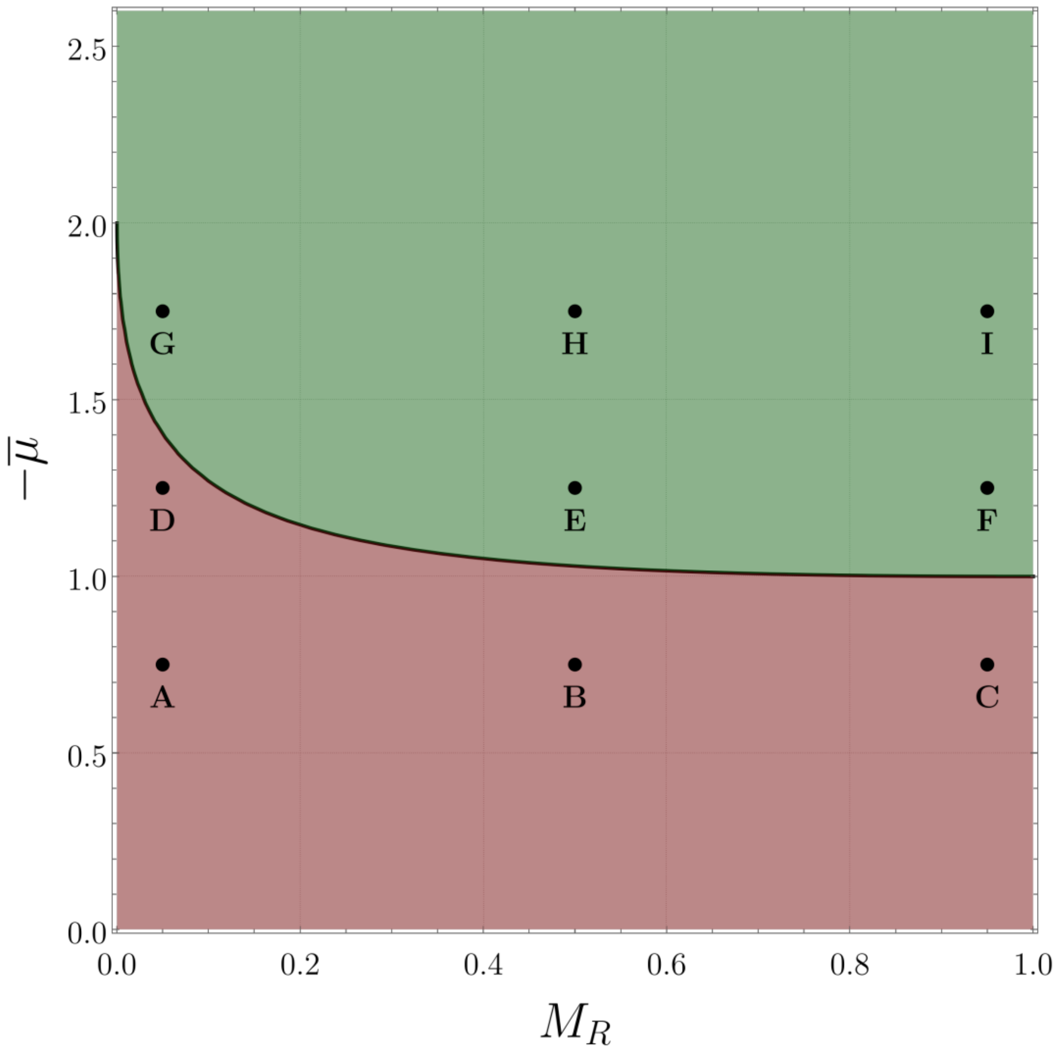


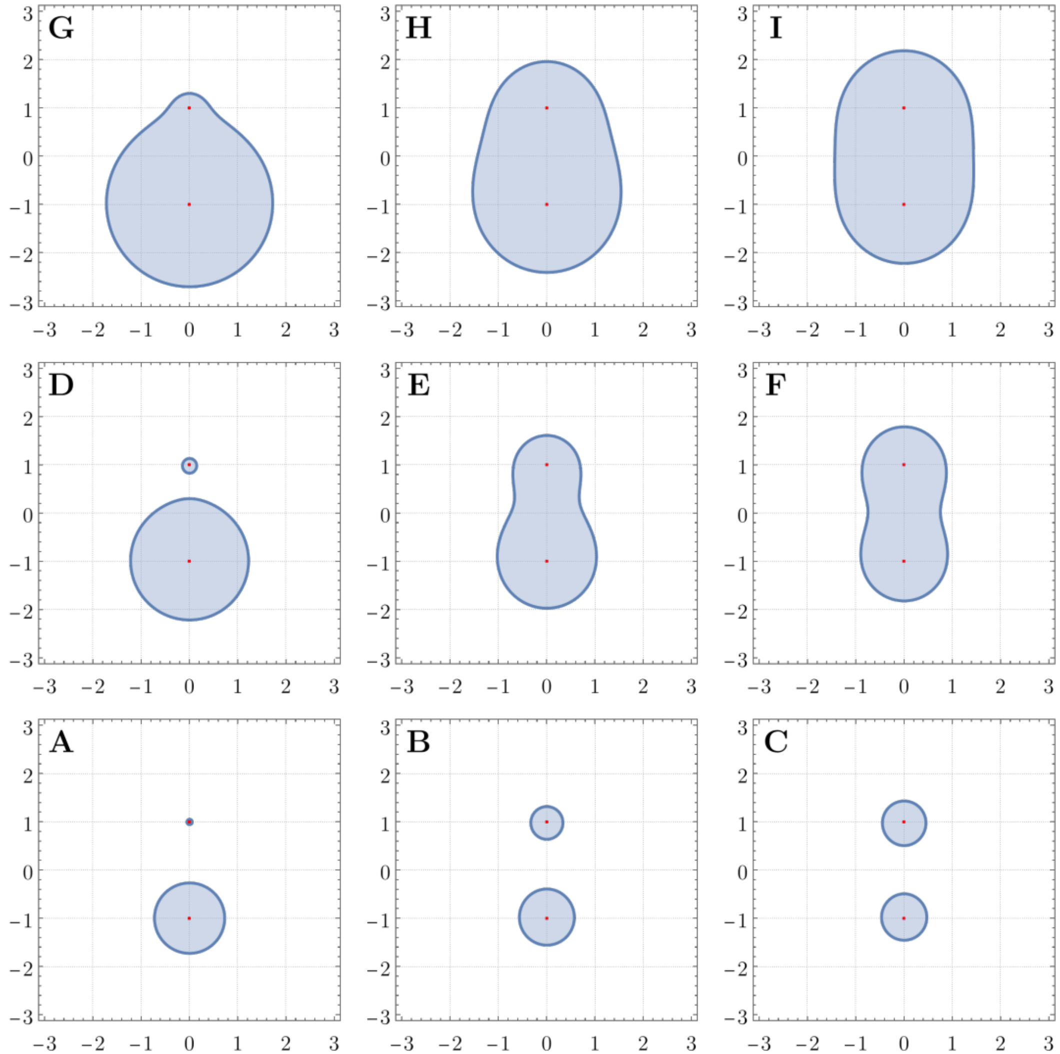

# The MP Penrose Process

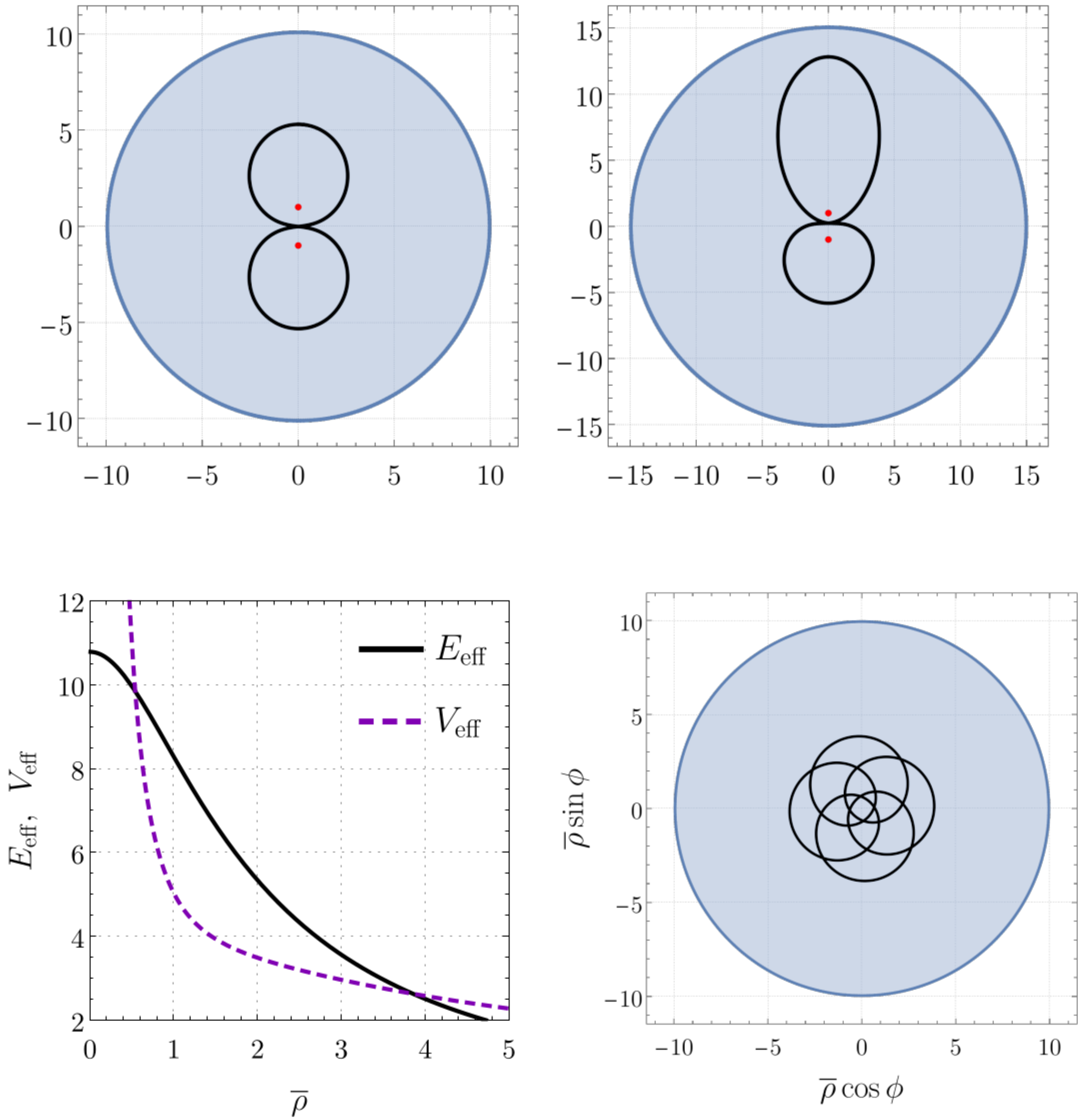


From the particle's energy equation, one can write

$$\dot{\rho}^2 + \dot{z}^2 = E_{\rm eff}^2(\rho, z) - V_{\rm eff}(\rho, z)$$

$$E_{\rm eff}(\rho, z) = E - \mu\left(1 - \frac{1}{U}\right)$$

$$V_{\rm eff}(\rho, z) = \frac{L^2}{\rho^2 U^4} + \frac{1}{U^2}$$

Where

$$E_{\rm eff}(\rho, z) \geq 0$$

$$E_{\rm eff}(\rho, z)^2 \geq V_{\rm eff}(\rho, z)$$

# The MP Penrose Process

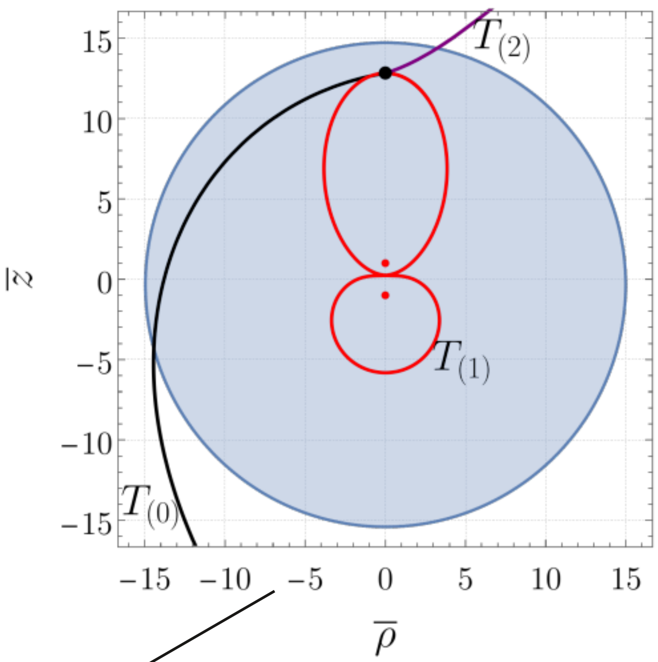


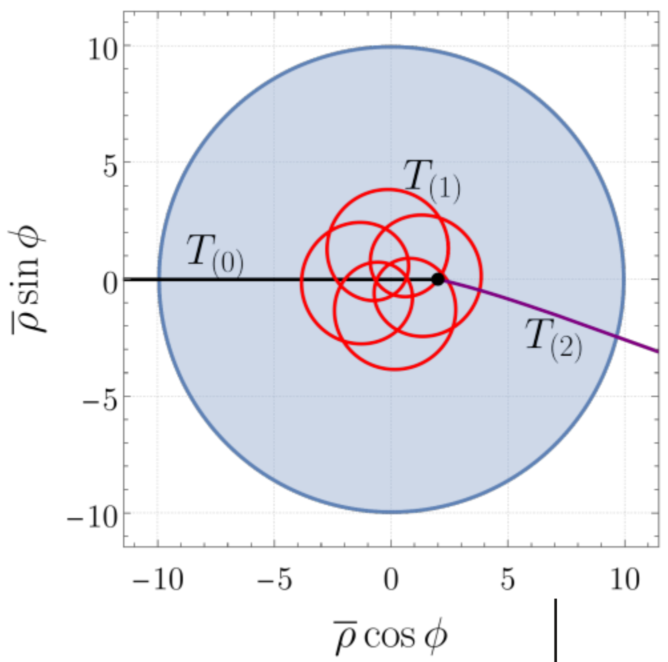


| $i$ | $m_{(i)}$ | $\mu_{(i)}$ | $E_{(i)}$ | $L_{(i)}$ | $\dot{\rho}_{(i)}$ | $\dot{z}_{(i)}$ |
|---|---|---|---|---|---|---|
| 0 | 1.00000 | -0.08345 | 1.00000 | 0 | 0.60000 | 0.09699 |
| 1 | 0.70000 | -5.00000 | -0.02000 | 0 | 0.41207 | 0.00000 |
| 2 | 0.23248 | 14.69629 | 4.36171 | 0 | 1.34012 | 0.41719 |

| $i$ | $m_{(i)}$ | $\mu_{(i)}$ | $E_{(i)}$ | $L_{(i)}$ | $\dot{\rho}_{(i)}$ | $\dot{z}_{(i)}$ |
|---|---|---|---|---|---|---|
| 0 | 1.00000 | -0.27698 | 1.00000 | 0.00000 | 1.00000 | 0 |
| 1 | 0.10000 | -5.00000 | -0.05000 | 12.85870 | 1.36059 | 0 |
| 2 | 0.33342 | 0.66890 | 3.01423 | -3.85662 | 2.59116 | 0 |

The Cabrera - Munguia, Manko and Ruiz solution (CMMR) describes two Kerr black holes held in static equilibrium by a massless strut (see Ref. [66])

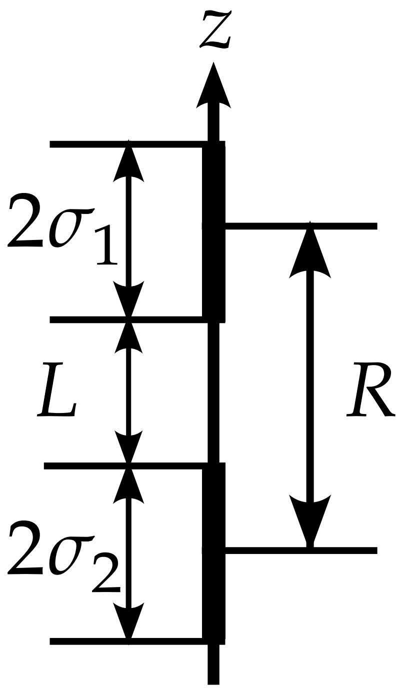


Adapted from Ref. [66]

$$\mathrm{d}s^2 = -f(\rho,z)\left[\mathrm{d}t - \omega(\rho,z)\mathrm{d}\phi\right]^2 + f(\rho,z)^{-1}\left[e^{2\gamma(\rho,z)}\left(\mathrm{d}\rho^2 + \mathrm{d}z^2\right) + \rho^2\mathrm{d}\phi^2\right]$$

$$a_{1,2} = M_{1,2}/J_{1,2}$$

$$M_T = M_1 + M_2$$

$$J_T = M_1 a_1 + M_2 a_2$$

$$\left(R^2 - M_T^2 + a_*^2\right)\left(a_1 + a_2 - a_*\right) + 2\left(R + M_T\right)\left(J_T - M_T a_*\right) = 0$$

# The CMMR Penrose Process

A charged particle, moving through this binary has energy given by

$$E = \frac{-f^2\omega L}{\rho^2-\omega^2 f^2} + \left[\frac{\rho^2 e^{2\gamma}(\dot{\rho}^2+\dot{z}^2)}{\rho^2-\omega^2 f^2} + \left(\frac{\rho f L}{\rho^2-\omega^2 f^2}\right)^2 + \frac{\rho^2 f}{\rho^2-\omega^2 f^2}\right]^{1/2}$$

This metric also possesses a global time-like Killing vector field. The ergosphere is the locus of all points where

$$f(\rho,z) > 0$$

# The CMMR Penrose Process

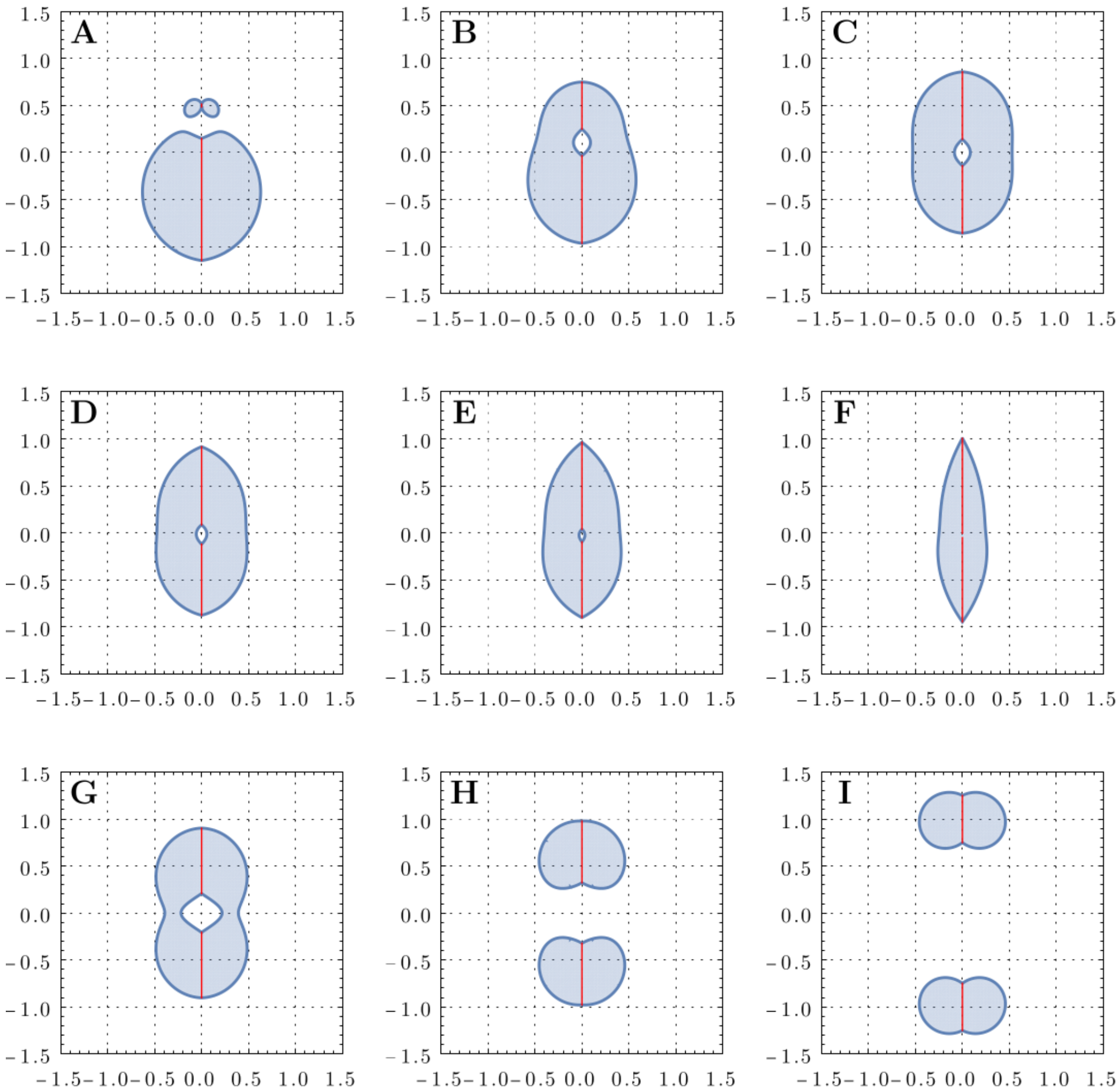


| Panel | $M_1/M_2$ | $a_1/M_T$ | $a_2/M_T$ | $R/M_T$ |
|---|---|---|---|---|
| **A** | 0.16 | 0.65 | 0.65 | 1.00 |
| **B** | 0.58 | 0.65 | 0.65 | 1.00 |
| **C** | 1.00 | 0.65 | 0.65 | 1.00 |
| **D** | 1.00 | 0.50 | 0.65 | 1.00 |
| **E** | 1.00 | 0.30 | 0.65 | 1.00 |
| **F** | 1.00 | −0.10 | 0.65 | 1.00 |
| **G** | 1.00 | 0.65 | 0.65 | 1.11 |
| **H** | 1.00 | 0.65 | 0.65 | 1.30 |
| **I** | 1.00 | 0.65 | 0.65 | 2.00 |

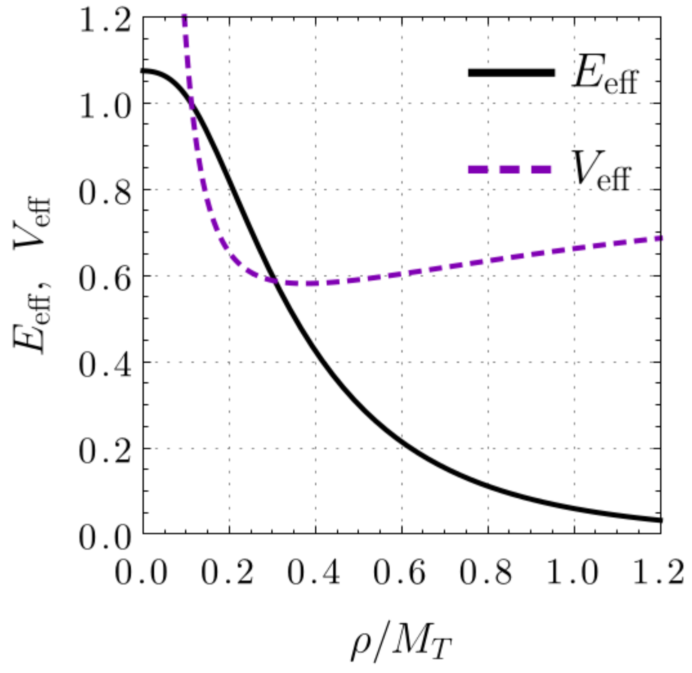


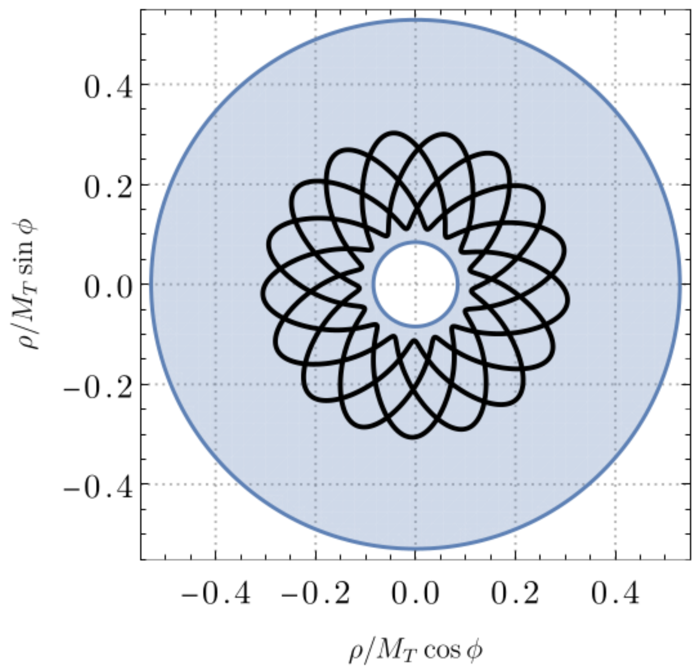


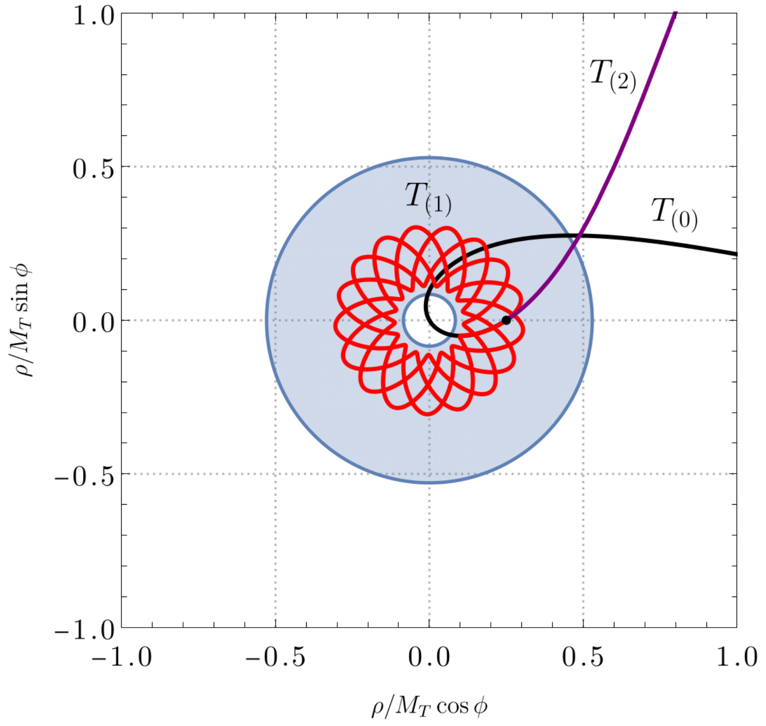


| $i$ | $m_{(i)}/m_0$ | $E_{(i)}$ | $L_{(i)}$ | $\dot{\rho}_{(i)}$ | $\dot{z}_{(i)}$ |
|---|---|---|---|---|---|
| 0 | 1.0000000 | 2.00000 | 0 .000000 | 4.343904 | 0 |
| 1 | 0.0289697 | -0.05400 | -2.500000 | 0.313887 | 0 |
| 2 | 0.3148980 | 6.35623 | 0.229993 | 13.765800 | 0 |

# Non-Stationary Penrose Process

So far, the PP depends on the existence of a conserved negative and "global" energy.

Let us relax this assumption. Our first step is to represent the spacetime of interest in 3+1 form.

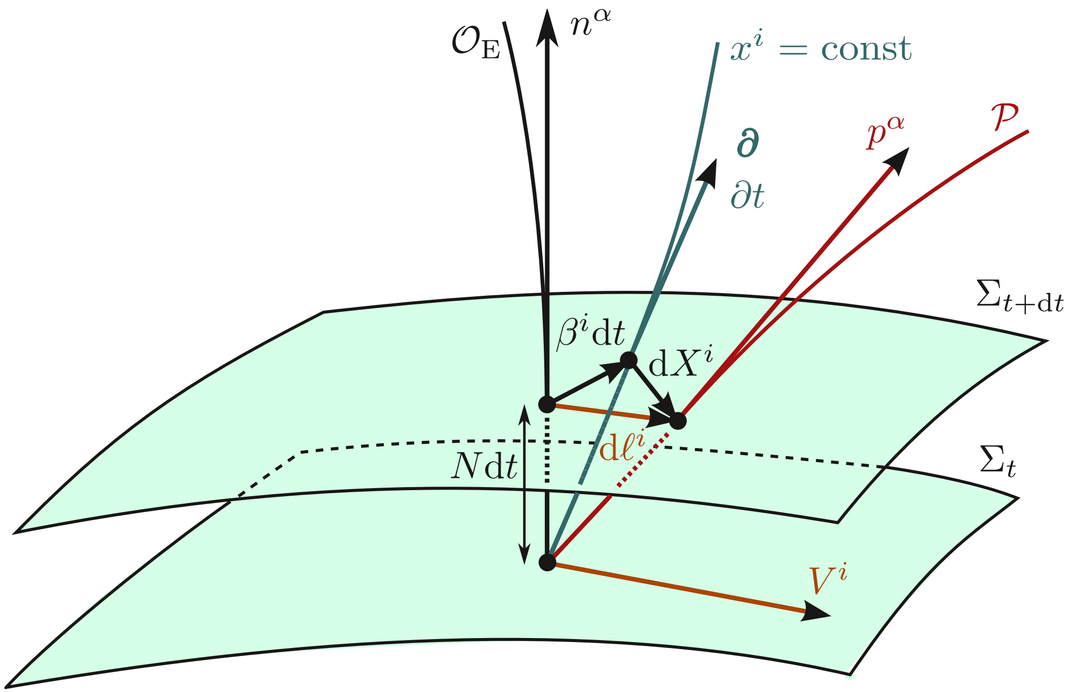


Extracted from Ref. [85]

$$\mathrm{d}s^2 = -N^2\mathrm{d}t^2 + \gamma_{ij}(\mathrm{d}x^i + \beta^i\mathrm{d}t)(\mathrm{d}x^j + \beta^j\mathrm{d}t).$$

# Non-Stationary Penrose Process

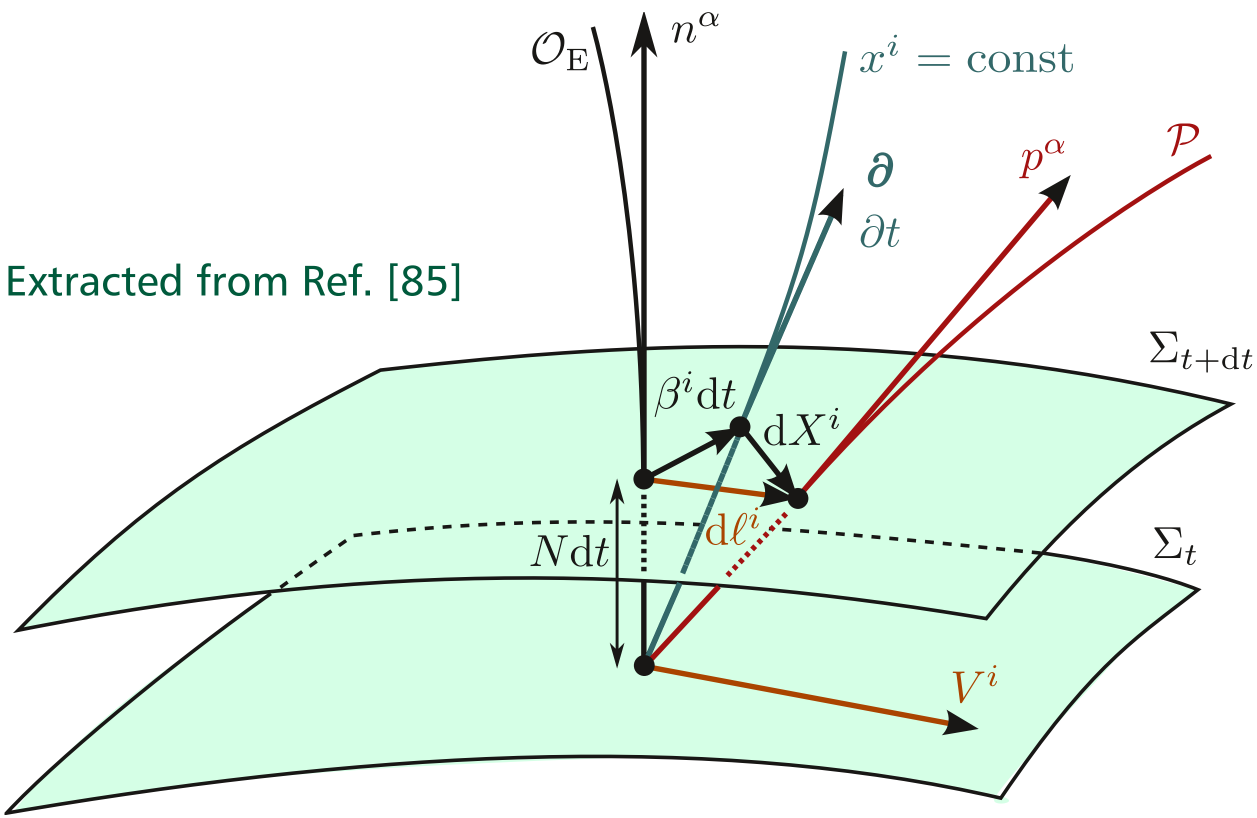


Extracted from Ref. [85]

$$p_\mu p^\mu = m^2\delta$$

$$p^\mu = E(n^\mu + V^\mu)$$

$$E = -n_\mu p^\mu \quad \text{(local)}$$

$$V_\mu V^\mu = V_i V^i = 1 + \delta\left(\frac{m}{E}\right)^2.$$

$$\frac{\mathrm{d}X^i}{\mathrm{d}t} = NV^i - \beta^i$$

$$\frac{\mathrm{d}V^i}{\mathrm{d}t} = NV^j\left[V^i\left(\partial_j \ln N - K_{jk}V^k\right) + 2K^i_{\ j} - {}^3\Gamma^i_{jk}V^k\right] - \gamma^{ij}\partial_j N - V^j\partial_j\beta^i$$

$$\frac{\mathrm{d}E}{\mathrm{d}t} = E(NK_{jk}V^jV^k - V^j\partial_j N)$$

# Non-Stationary Penrose Process

We define the global energy

$$\varepsilon = -p_\mu \xi^\mu$$

Where

$$\xi^\mu = (\partial_t)^\mu$$

We can bridge the two energy definitions by using the four-momentum decomposition and the general 3+1 decomposed metric

$$\varepsilon = (N - \gamma_{ij}\beta^i V^j)E$$

# Non-Stationary Penrose Process

$$\varepsilon = (N - \gamma_{ij}\beta^i V^j)E$$

When $\varepsilon$ represents a global time-like Killing vector field, $\xi^\mu$ can be interpreted as a conserved energy along a particle's trajectory. In general, though, this is not true.

Note, however, that if the spacetime metric is asymptotically flat, both definitions coincide at spatial infinity. Furthermore, at infinity, global energy is again physically meaningful.

This means that even though we cannot use global energy to make physical statements close to a gravitational center, we can do so at infinity.

# Non-Stationary Penrose Process

$$\varepsilon = (N - \gamma_{ij}\beta^i V^j)E$$

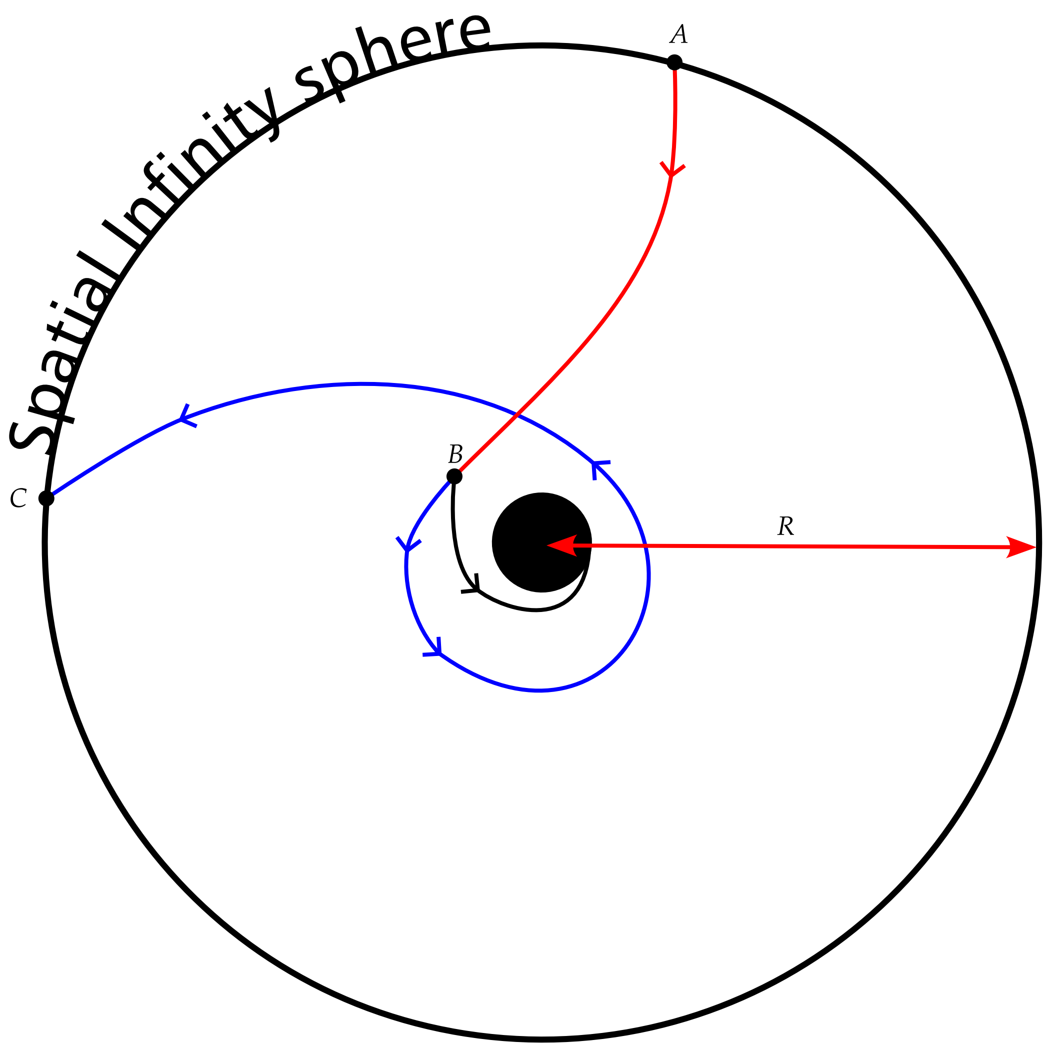


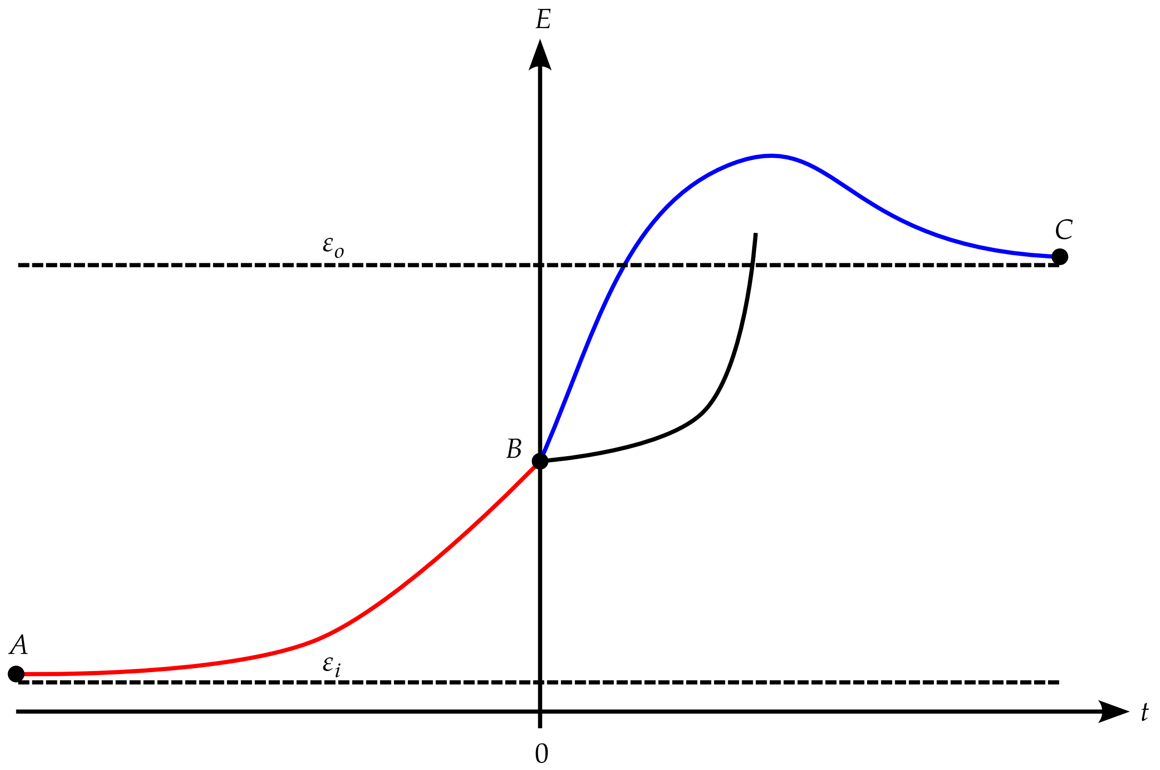

# Non-Stationary Penrose Process

## Proof of concept: Kerr spacetime in KS coordinates

| $E(0)$ | $m$ |
|---|---|
| 1.0 | $1.0 \times 10^{-1}$ |
| $8.0 \times 10^{-3}$ | $1.0 \times 10^{-4}$ |
| $9.9199999999999999 \times 10^{-1}$ | $9.5800493929138735 \times 10^{-3}$ |

| $V^x(0)$ | $V^y(0)$ |
|---|---|
| 0.6769503786998466 | 0.6740022058848380 |
| 0.5948571400034293 | −0.3343724878526367 |
| 0.67761242094739838 | 0.68213425986659171 |

| $E(t_f)$ | $\varepsilon(t_f)$ | $\lvert E(t_f) - \varepsilon(t_f)\rvert$ |
|---|---|---|
| $3.8435595988010596 \times 10^{-1}$ | $3.8435613882134312 \times 10^{-1}$ | $1.7894123710560095 \times 10^{-7}$ |
| $3.8515962539170862 \times 10^{-1}$ | $3.8515904777176790 \times 10^{-1}$ | $5.776199407114824 \times 10^{-7}$ |

| | |
|---|---|
| $E_{\text{out}}(t_f) - E_{\text{in}}(t_f)$ | 0.0008036655116026026 |
| $\varepsilon_{\text{out}}(t_f) - \varepsilon_{\text{in}}(t_f)$ | 0.0008029089504247855 |
| $\eta_E$ | 0.0020909406786700896 |
| $\eta_\varepsilon$ | 0.0020889722919224165 |

# Non-Stationary Penrose Process

## Proof of concept: SKS spacetime

$$g_{\mu\nu}(t,x,y,z) = \eta_{\mu\nu} + \overline{\mathcal{H}}^{(1)}_{\mu\nu} + \overline{\mathcal{H}}^{(2)}_{\mu\nu} \quad (T^{(i)},X^{(i)},Y^{(i)},Z^{(i)}) \to \overline{M}^{(i)}_{\mu\nu} \equiv \overline{\mathcal{H}}^{(i)}_{\mu\nu}(t,x,y,z) \quad \overline{M}^{(i)}_{\mu\nu} = H^{(i)}\Lambda^{(i)\alpha}{}_{\mu}\Lambda^{(i)\beta}{}_{\nu}l^{(i)}_{\alpha}l^{(i)}_{\beta}$$

| $V^x(0)$ | $V^y(0)$ |
|---|---|
| 0.6769503786998466 | 0.6740022058848380 |
| 0.5948571400034293 | −0.3343724878526367 |
| 0.66011565390809868 | 0.68380243736284951 |

| $E(0)$ | $m$ |
|---|---|
| 1.0 | $1.0 \times 10^{-1}$ |
| $8.0 \times 10^{-3}$ | $1.0 \times 10^{-4}$ |
| $9.9199999999999999 \times 10^{-1}$ | $9.5800493929022838 \times 10^{-3}$ |

| $E(t_f)$ | $\varepsilon(t_f)$ | $\lvert E(t_f) - \varepsilon(t_f)\rvert$ |
|---|---|---|
| $2.4452985315377770 \times 10^{-1}$ | $2.4453006741751246 \times 10^{-1}$ | $2.1426373481014949 \times 10^{-7}$ |
| $3.4638508542318119 \times 10^{-1}$ | $3.4638400572434974 \times 10^{-1}$ | $1.0796988314520917 \times 10^{-6}$ |

| | |
|---|---|
| $E_{\text{out}}(t_f) - E_{\text{in}}(t_f)$ | 0.10185523226940352 |
| $\varepsilon_{\text{out}}(t_f) - \varepsilon_{\text{in}}(t_f)$ | 0.10185393830683726 |
| $\eta_E$ | 0.41653495863897544 |
| $\eta_\varepsilon$ | 0.41652966700464295 |

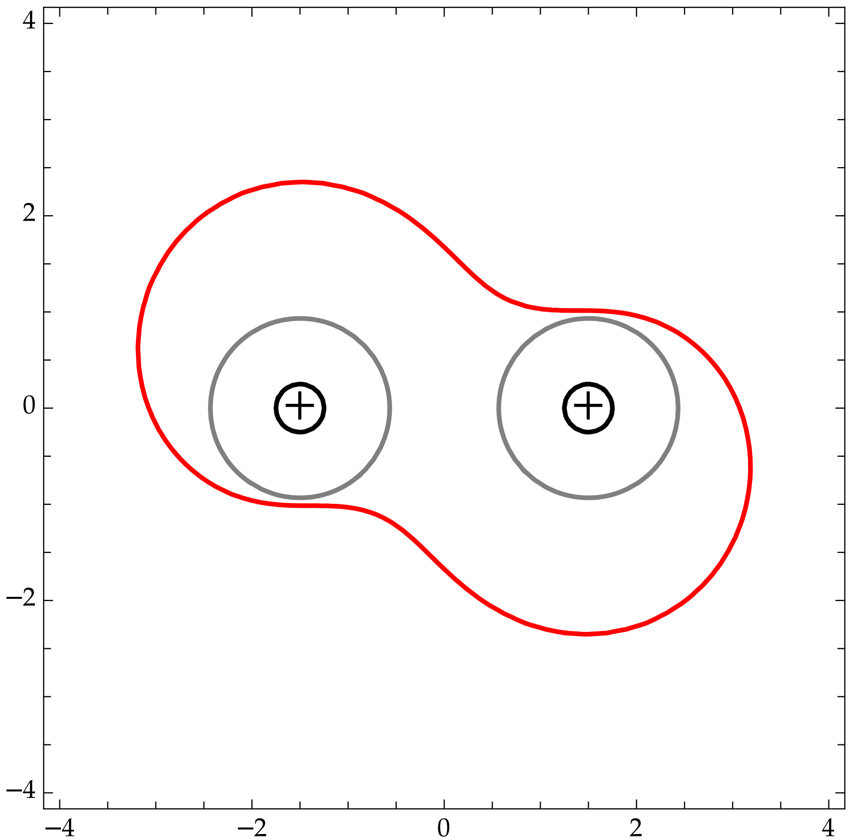

# Simulating Wave Scattering in GW150914

We wished to study scalar perturbation on top of an arbitrary background without backreaction.

The governing system of equations is

$$\partial_t \Phi = -2\alpha K_\phi + \mathcal{L}_\beta \Phi$$

$$\partial_t K_\Phi = \alpha \left( K K_\Phi - \tfrac{1}{2} \gamma^{ij} D_i \partial_j \Phi + \tfrac{1}{2} \mu^2 \Phi \right) - \tfrac{1}{2} \gamma^{ij} \partial_i \alpha \partial_j \Phi + \mathcal{L}_\beta K_\Phi$$

$$K_\Phi = -\tfrac{1}{2\alpha} \left( \partial_t - \mathcal{L}_\beta \right) \Phi$$

This system was implemented as a Thorn in the Einstein Toolkit

# Simulating Wave Scattering in GW150914

## Difficulties in 3D simulations

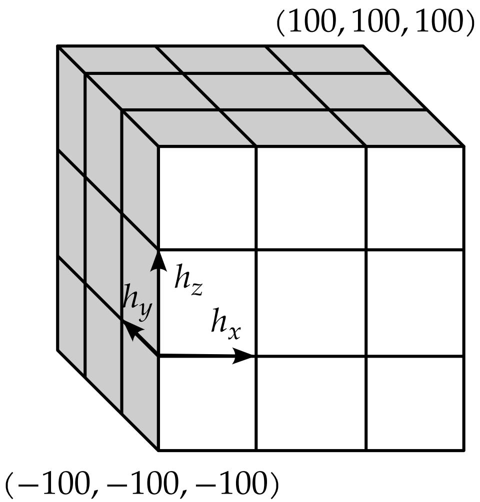


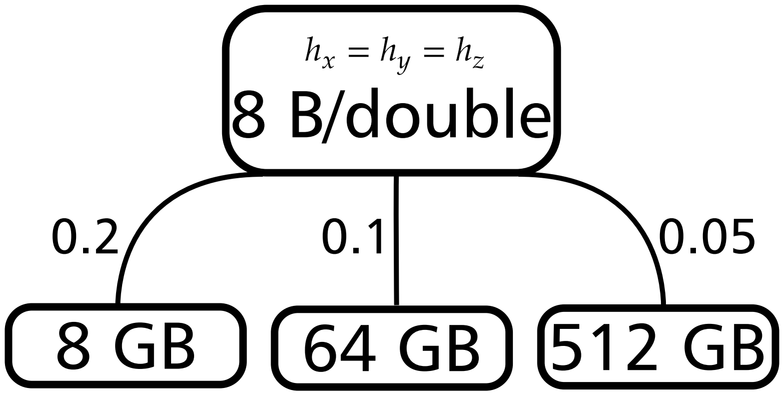


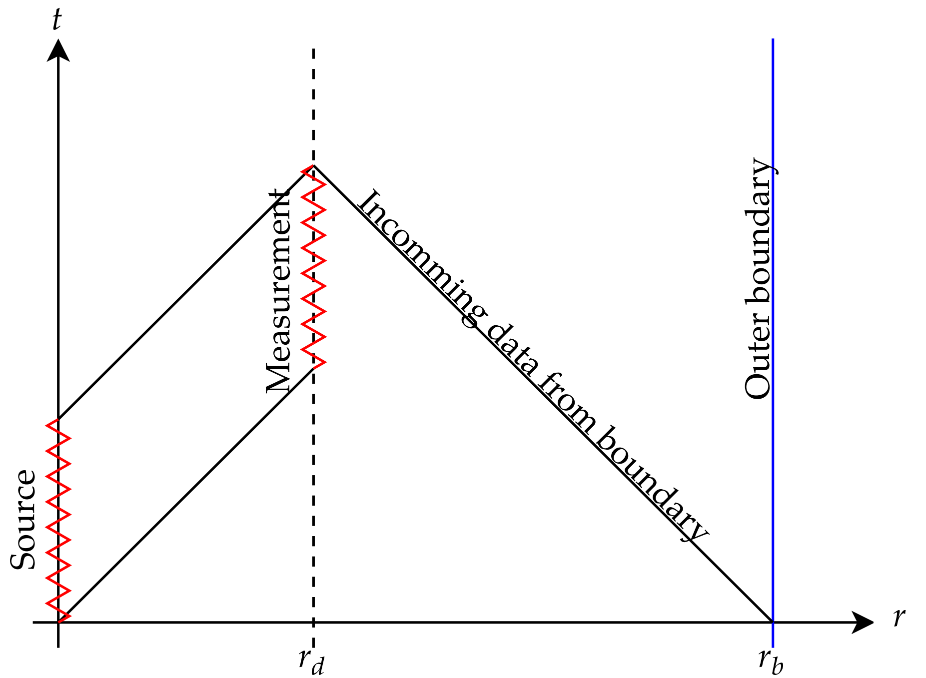


Adapeted from Ref. [2]

# Simulating Wave Scattering in GW150914

## Solution: Multipatch system via Llama

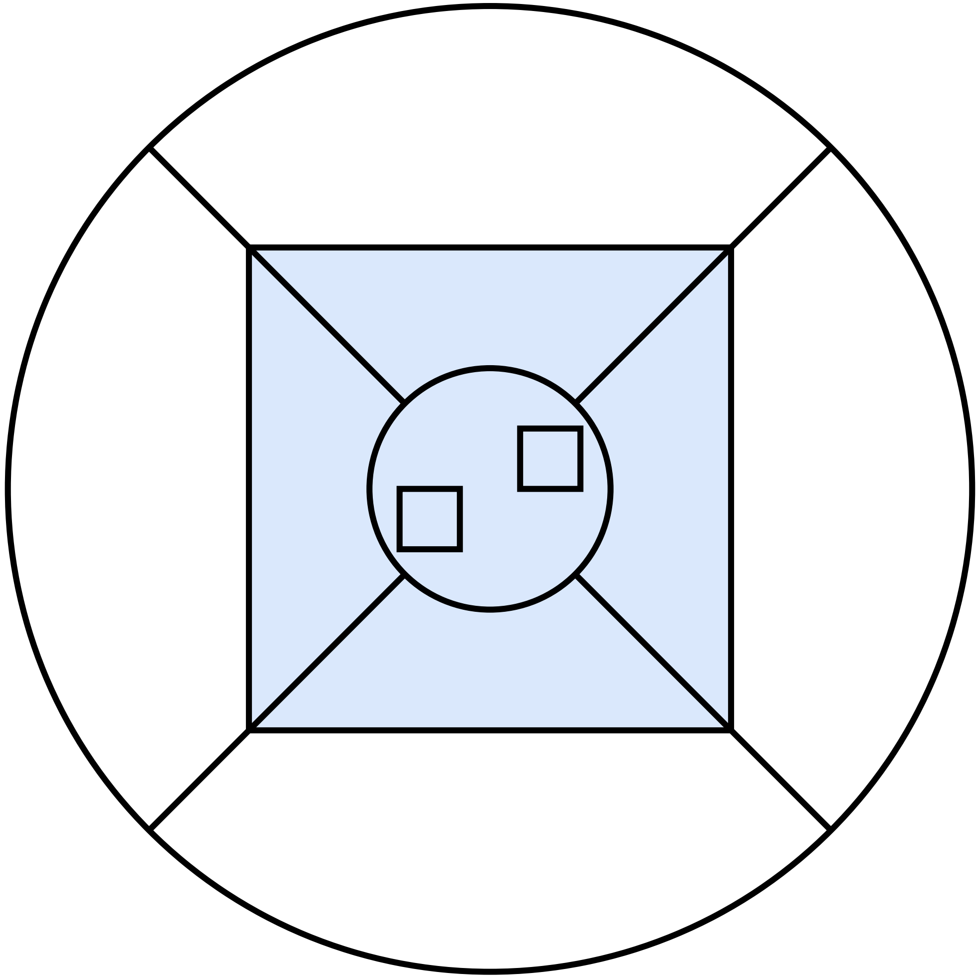

# Simulating Wave Scattering in GW150914

## Plane wave initial data

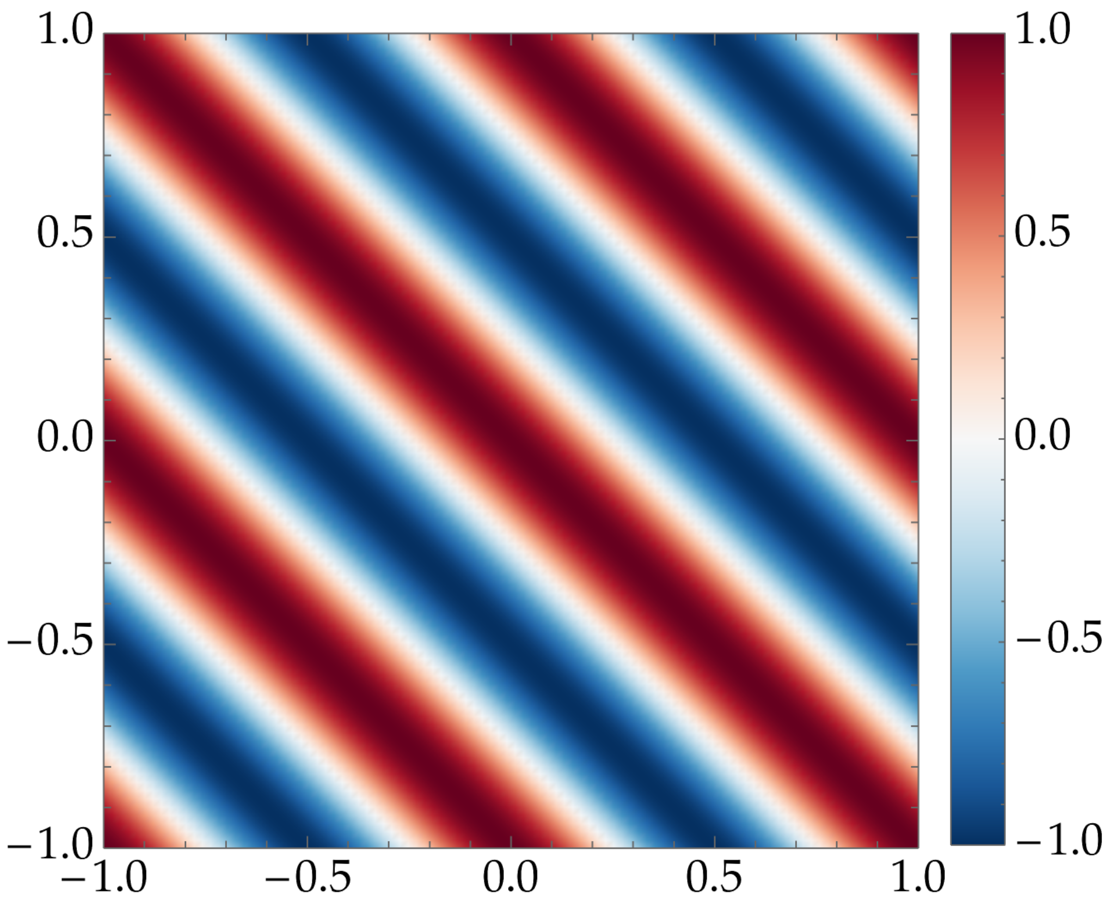


$$P_w(t,x,y,z) = \cos\omega$$

$$\Omega = \sqrt{K_x^2 + K_y^2 + K_z^2}$$

$$n_t = \Omega(t - t_0)$$

$$n_x = K_x(x - x_0)$$

$$n_y = K_y(y - y_0)$$

$$n_z = K_z(z - z_0)$$

$$\omega = 2\pi\left(n_t + n_x + n_y + n_z\right)$$

# Simulating Wave Scattering in GW150914

## Exact Gaussian initial data

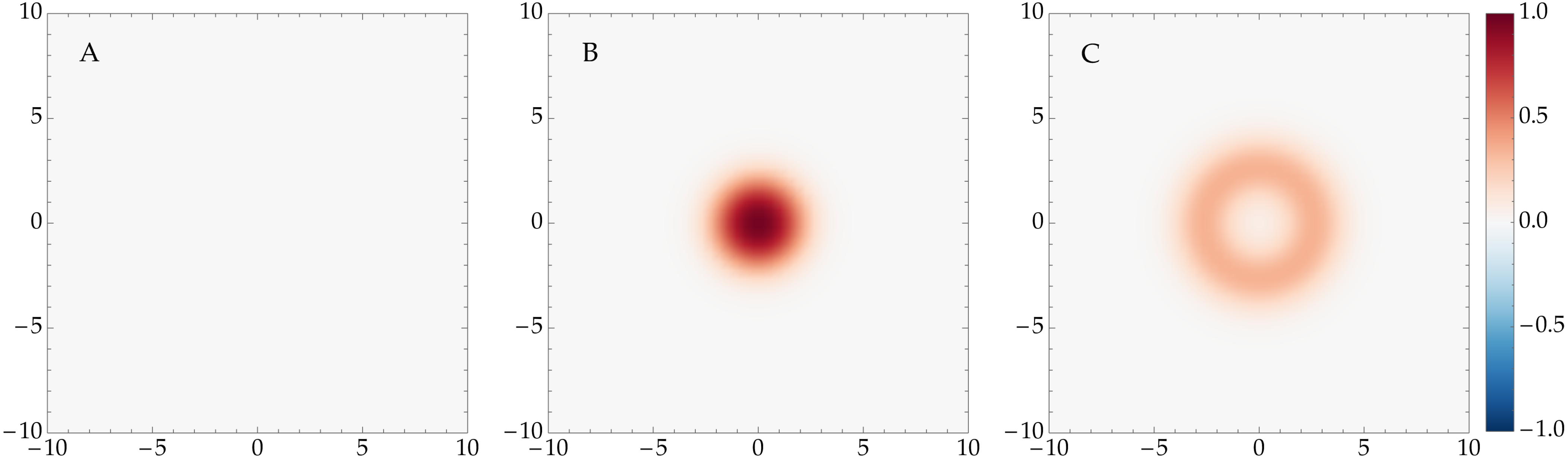


$$G(r,\sigma) = \exp\left(-\frac{1}{2}\left(\frac{r}{\sigma}\right)^2\right)$$

$$E_G(t,r,\sigma) = \left(G(r-t,\sigma) - G(r+t,\sigma)\right)/r$$

# Simulating Wave Scattering in GW150914

## Multipolar Gaussian Initial Data

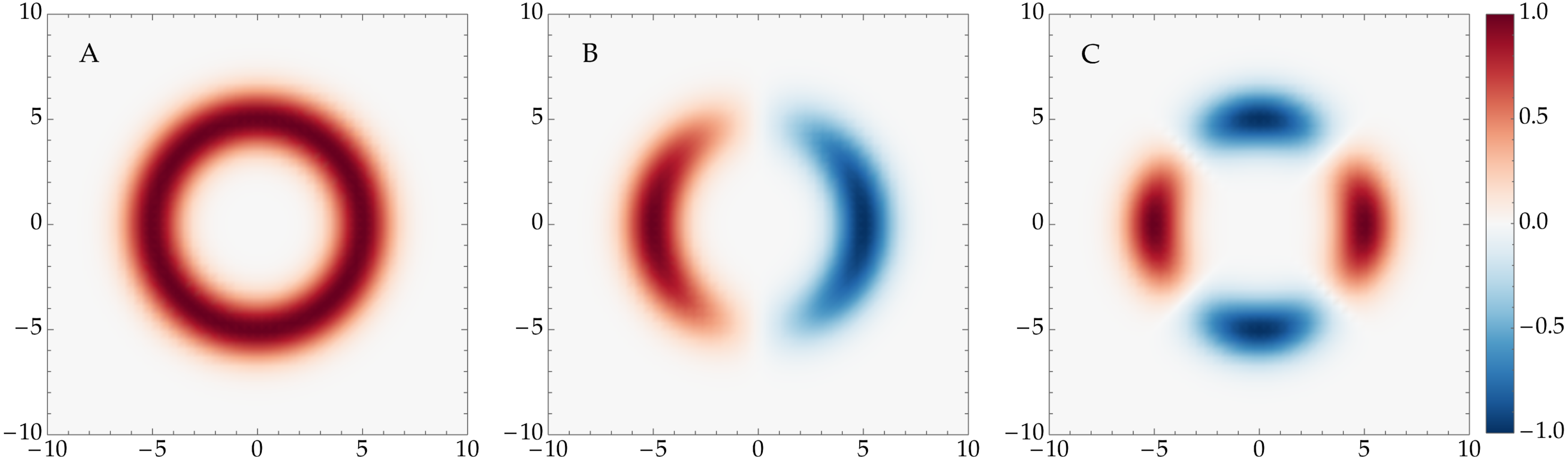


$$M_G(x,y,z) = \sum_{l=0}^{N} \sum_{m=-l}^{l} c_{lm} Y_{lm}(X,Y,Z) G(R - R_0, \sigma)$$

$$X \equiv x - x_0$$

$$Y \equiv y - y_0$$

$$Z \equiv z - z_0$$

$$R \equiv \sqrt{X^2 + Y^2 + Z^2}$$

# Simulating Wave Scattering in GW150914

## Preliminary Evolution results

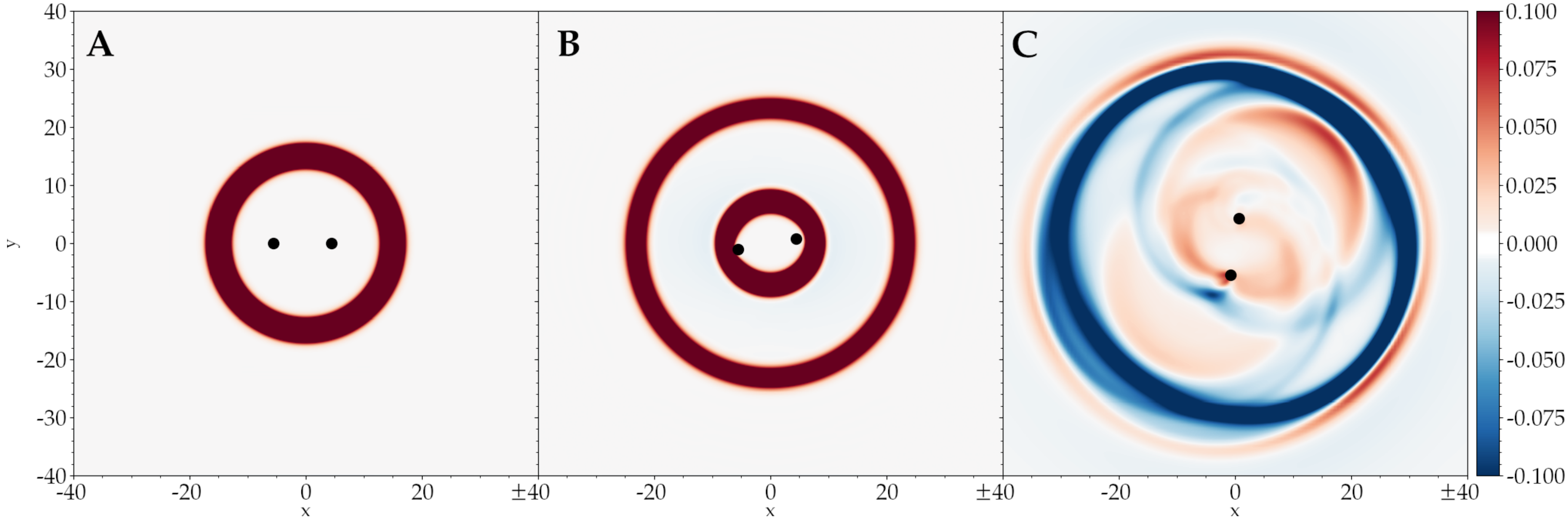

# Preliminary Evolution results

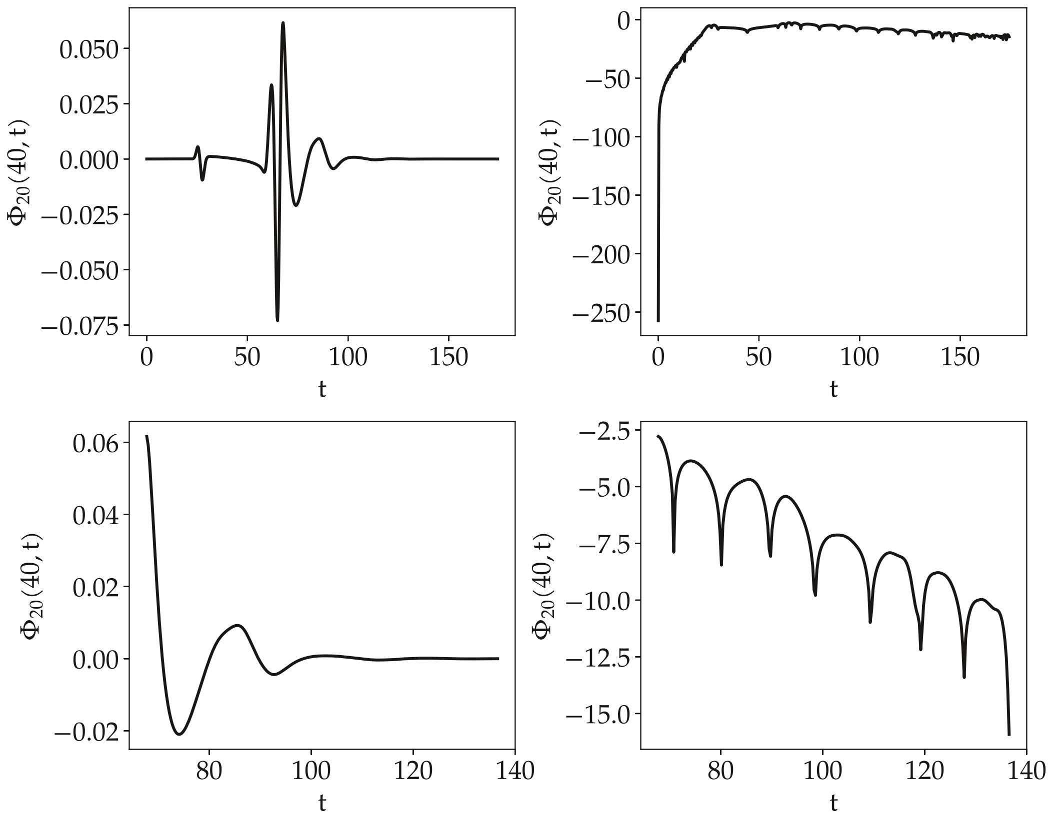


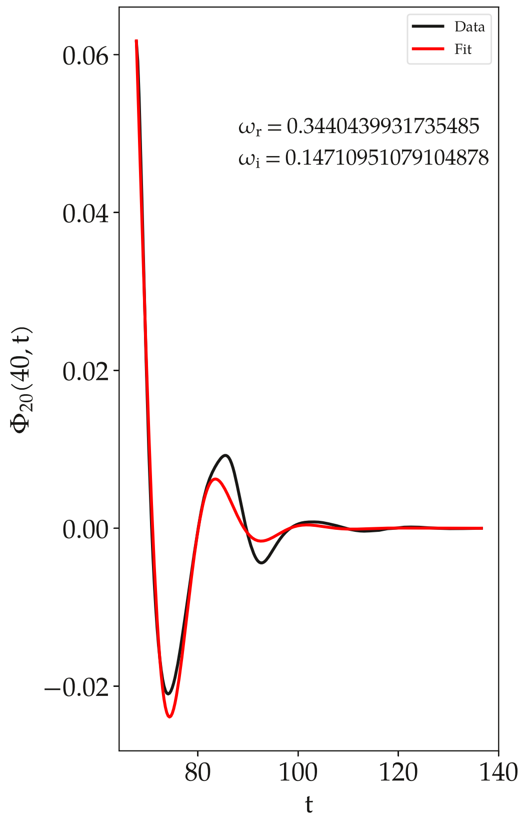


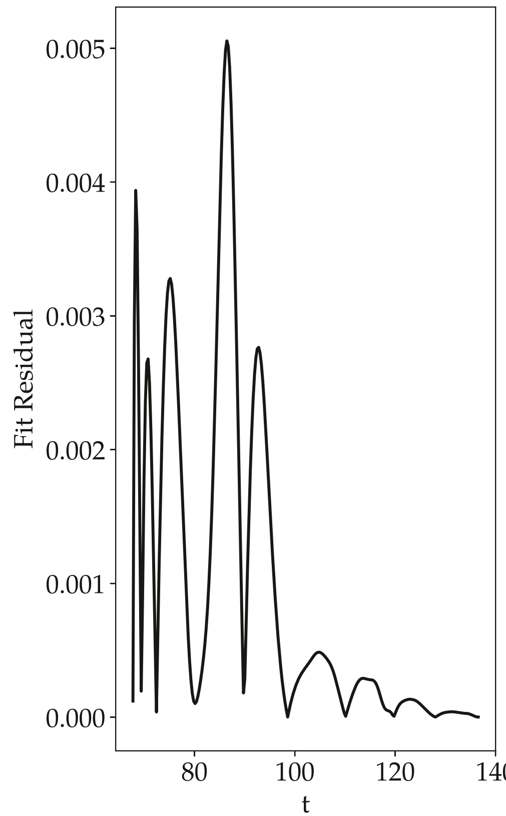

## Preliminary Evolution results

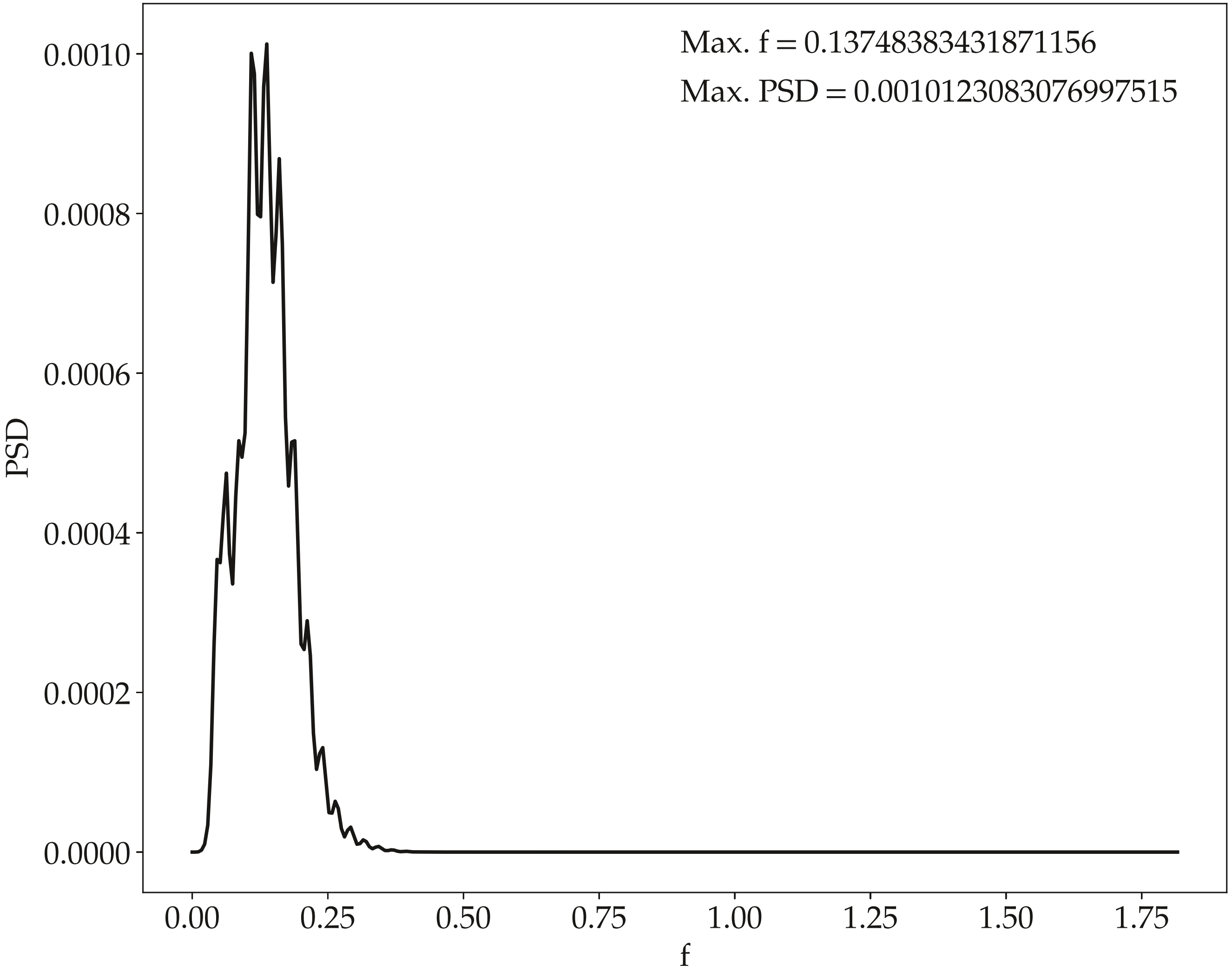

# The AIM and QuasinormalModes.jl

The differential equation

$$y^{(2)}(x) - \lambda_0(x)y^{(1)}(x) - s_0(x)y(x) = 0$$

has a solution of the form

$$y(x) = \exp\left(-\int^x \alpha \mathrm{d}t\right)\left\{C_2 + C_1 \int^x \exp\left[\int^t (\lambda_0(\tau) + 2\alpha(\tau))\mathrm{d}\tau\right]\mathrm{d}t\right\}$$

if for some positive n

$$\alpha(x) \equiv \frac{s_n(x)}{\lambda_n(x)} = \frac{s_{n-1}(x)}{\lambda_{n-1}(x)} \qquad \delta(x) \equiv s_n(x)\lambda_{n-1}(x) - \lambda_n(x)s_{n-1}(x) = 0$$

is satisfied, where

$$\lambda_k(x) \equiv \lambda_{k-1}^{(1)}(x) + s_{k-1}(x) + \lambda_0(x)\lambda_{k-1}(x) \qquad s_k(x) \equiv s_{k-1}^{(1)}(x) + s_0(x)\lambda_{k-1}(x)$$

The method converges if

$$\lim_{n\to\infty} \frac{\delta_n(x)}{\lambda_{n-1}^2(x)} = 0$$

# The AIM and QuasinormalModes.jl

Each iteration requires recursive derivatives of previous iterations. This is computationally challenging and can generate untreatable expressions quickly.

We can mitigate this by using a Taylor expansion of the coefficients around some arbitrary point

$$\lambda_n(\xi) = \sum_{i=0}^{\infty} c_n^i (x-\xi)^i$$

$$s_n(\xi) = \sum_{i=0}^{\infty} d_n^i (x-\xi)^i,$$

This leads to a new quantization condition and coefficient "rules"

$$\delta \equiv d_n^0 c_{n-1}^0 - d_{n-1}^0 c_n^0 = 0 \qquad c_n^i = (i+1)c_{n-1}^{i+1} + d_{n-1}^i + \sum_{k=0}^{i} c_0^k c_{n-1}^{i-k} \qquad d_n^i = (i+1)d_{n-1}^{i+1} + \sum_{k=0}^{i} d_0^k c_{n-1}^{i-k}.$$

# The AIM and QuasinormalModes.jl

$$\begin{pmatrix} c_0^0 & c_1^0 & c_2^0 \\ c_0^1 & c_1^1 & c_2^1 \\ c_0^2 & c_1^2 & c_2^2 \end{pmatrix} \begin{pmatrix} d_0^0 & d_1^0 & d_2^0 \\ d_0^1 & d_1^1 & d_2^1 \\ d_0^2 & d_1^2 & d_2^2 \end{pmatrix}$$

$$\begin{pmatrix} c_0^0 & c_1^0 & c_2^0 \\ c_0^1 & c_1^1 & c_2^1 \\ c_0^2 & c_1^2 & c_2^2 \end{pmatrix} \begin{pmatrix} d_0^0 & d_1^0 & d_2^0 \\ d_0^1 & d_1^1 & d_2^1 \\ d_0^2 & d_1^2 & d_2^2 \end{pmatrix}$$

$$\begin{pmatrix} c_0^0 & c_1^0 & c_2^0 \\ c_0^1 & c_1^1 & c_2^1 \\ c_0^2 & c_1^2 & c_2^2 \end{pmatrix} \begin{pmatrix} d_0^0 & d_1^0 & d_2^0 \\ d_0^1 & d_1^1 & d_2^1 \\ d_0^2 & d_1^2 & d_2^2 \end{pmatrix}$$

$$\begin{pmatrix} d_0^0 & d_1^0 & d_2^0 \\ d_0^1 & d_1^1 & d_2^1 \\ d_0^2 & d_1^2 & d_2^2 \end{pmatrix} \begin{pmatrix} c_0^0 & c_1^0 & c_2^0 \\ c_0^1 & c_1^1 & c_2^1 \\ c_0^2 & c_1^2 & c_2^2 \end{pmatrix}$$

$$\begin{pmatrix} d_0^0 & d_1^0 & d_2^0 \\ d_0^1 & d_1^1 & d_2^1 \\ d_0^2 & d_1^2 & d_2^2 \end{pmatrix} \begin{pmatrix} c_0^0 & c_1^0 & c_2^0 \\ c_0^1 & c_1^1 & c_2^1 \\ c_0^2 & c_1^2 & c_2^2 \end{pmatrix}$$

$$\begin{pmatrix} d_0^0 & d_1^0 & d_2^0 \\ d_0^1 & d_1^1 & d_2^1 \\ d_0^2 & d_1^2 & d_2^2 \end{pmatrix} \begin{pmatrix} c_0^0 & c_1^0 & c_2^0 \\ c_0^1 & c_1^1 & c_2^1 \\ c_0^2 & c_1^2 & c_2^2 \end{pmatrix}$$

# The AIM and QuasinormalModes.jl

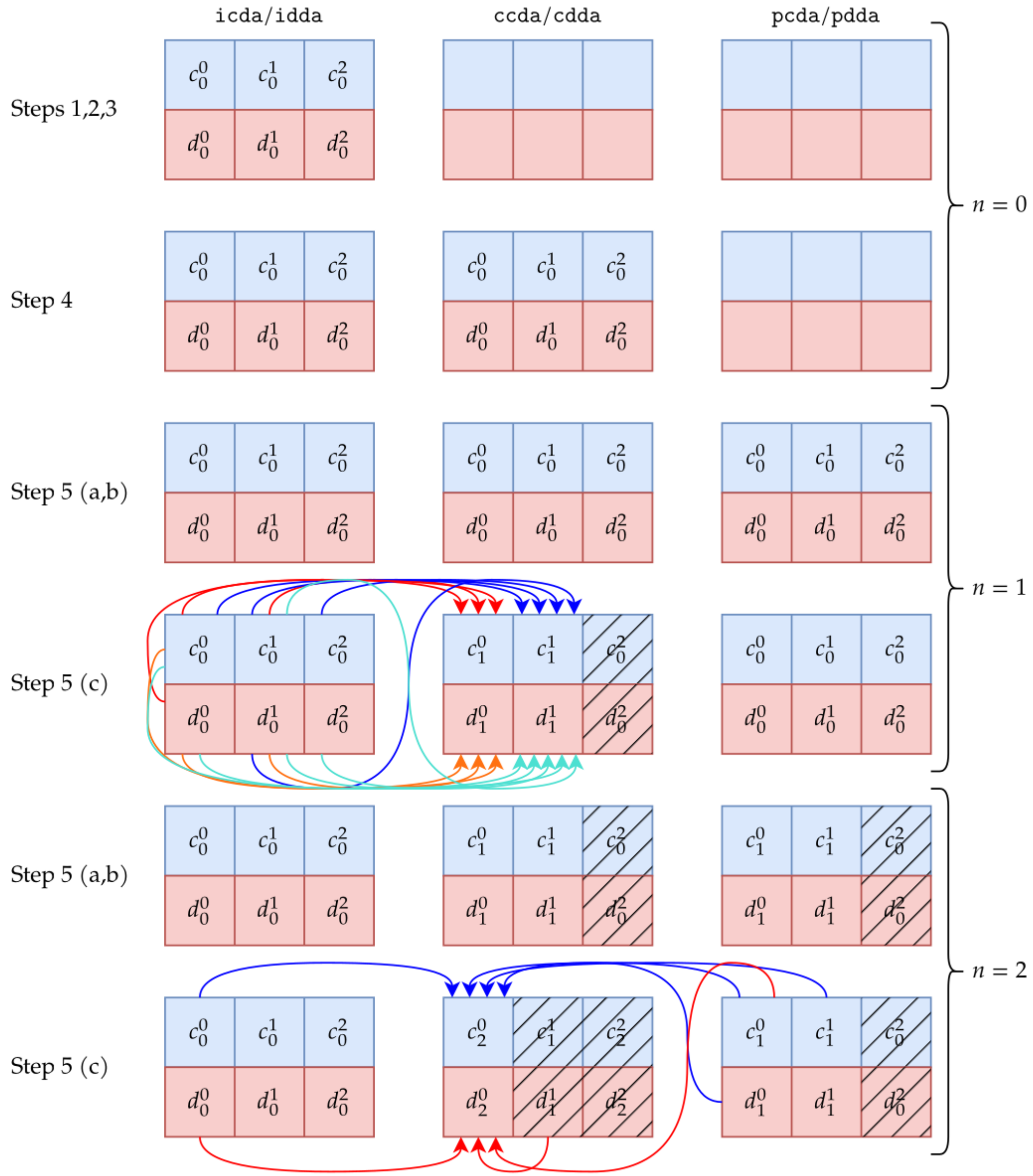

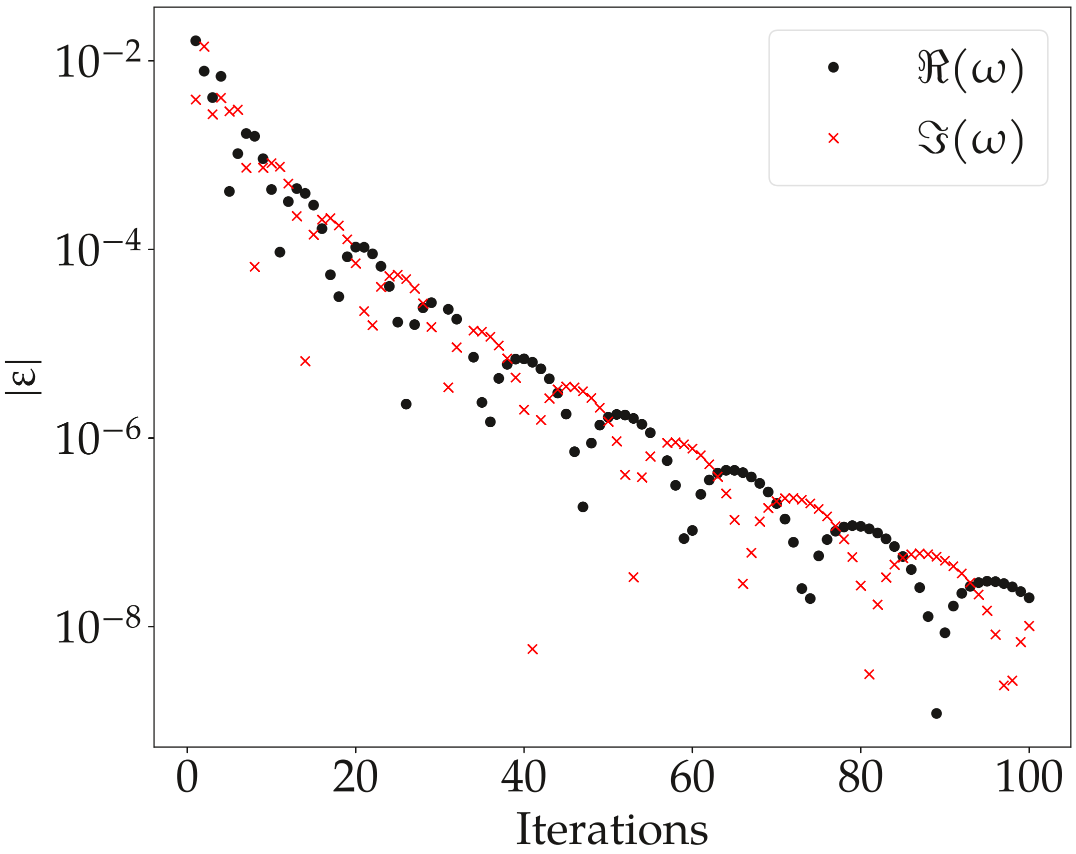
$|\varepsilon|$
$10^{-2}$
$10^{-4}$
$10^{-6}$
$10^{-8}$
0
20
40
60
80
100
Iterations
$\Re(\omega)$
$\Im(\omega)$

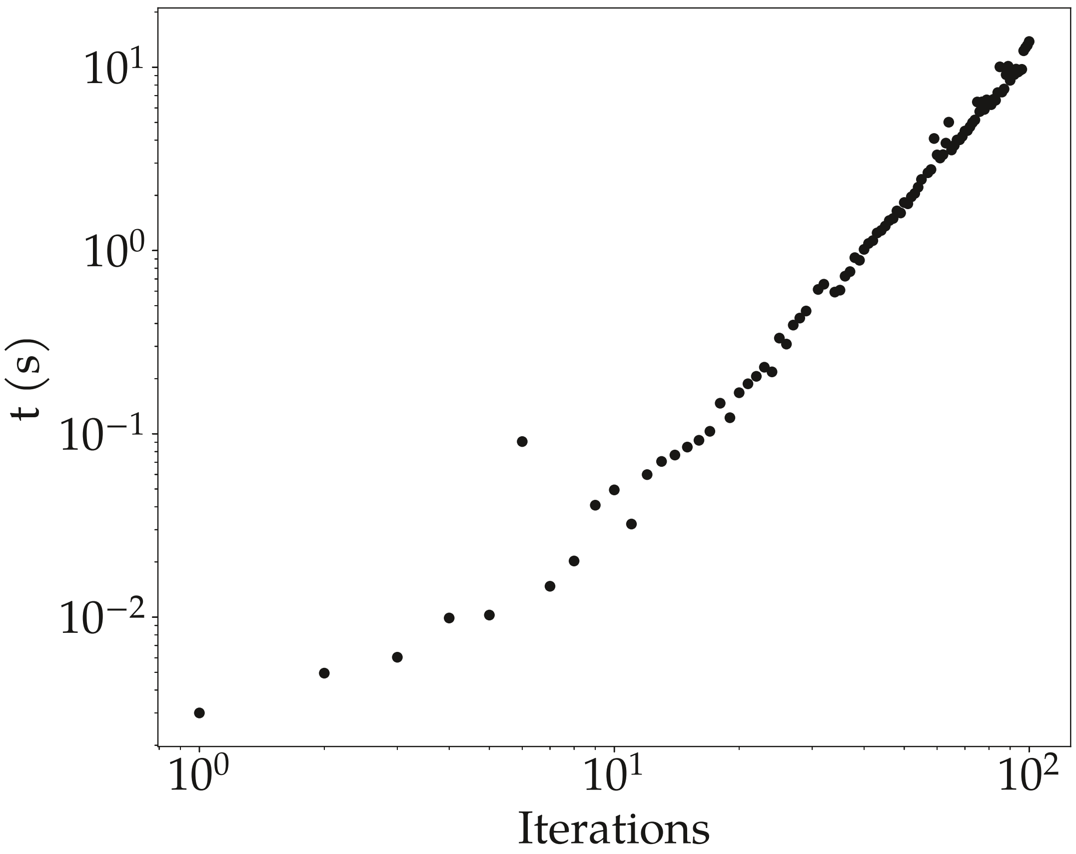
t (s)
$10^{1}$
$10^{0}$
$10^{-1}$
$10^{-2}$
$10^{0}$
$10^{1}$
$10^{2}$
Iterations

# The AIM and QuasinormalModes.jl

| $l$ | $n$ | Pseudo-spectral I (60 Polynomials) | Pseudo-spectral II (40 polynomials) | AIM 100 Iterations |
|---|---|---|---|---|
| 0 | 0 | $\pm 0.462727 - 0.092578i$ | $\pm 0.462727 - 0.092578i$ | $0.462727 - 0.092577i$ |
| 1 | 0 | $\pm 0.687103 - 0.094566i$ | $\pm 0.687103 - 0.094566i$ | $0.687103 - 0.094566i$ |
| | 1 | $\pm 0.670542 - 0.285767i$ | $\pm 0.670542 - 0.285767i$ | $0.670542 - 0.285767i$ |
| 2 | 0 | $\pm 0.897345 - 0.095309i$ | $\pm 0.897345 - 0.095309i$ | $0.897345 - 0.095309i$ |
| | 1 | $\pm 0.884980 - 0.287266i$ | $\pm 0.884980 - 0.287266i$ | $0.884980 - 0.287266i$ |
| | 2 | $\pm 0.861109 - 0.483113i$ | $\pm 0.861109 - 0.483113i$ | $0.861109 - 0.483113i$ |
| 3 | 0 | $\pm 1.101190 - 0.095648i$ | $\pm 1.101190 - 0.095648i$ | $1.101190 - 0.095648i$ |
| | 1 | $\pm 1.091300 - 0.287886i$ | $\pm 1.091300 - 0.287886i$ | $1.091300 - 0.287886i$ |
| | 2 | $\pm 1.071999 - 0.482895i$ | $\pm 1.071999 - 0.482895i$ | $1.071999 - 0.482895i$ |
| | 3 | $\pm 1.044272 - 0.682307i$ | $\pm 1.044272 - 0.682307i$ | $1.044272 - 0.682307i$ |
| 4 | 0 | $\pm 1.301587 - 0.095829i$ | $\pm 1.301587 - 0.095829i$ | $1.301587 - 0.095829i$ |
| | 1 | $\pm 1.293328 - 0.288184i$ | $\pm 1.293328 - 0.288184i$ | $1.293328 - 0.288184i$ |
| | 2 | $\pm 1.277107 - 0.482604i$ | $\pm 1.277107 - 0.482604i$ | $1.277107 - 0.482604i$ |
| | 3 | $\pm 1.253526 - 0.680366i$ | $\pm 1.253526 - 0.680366i$ | $1.253526 - 0.680366i$ |
| | 4 | $\pm 1.223513 - 0.882554i$ | $\pm 1.223512 - 0.882553i$ | $1.223513 - 0.882554i$ |

| Pseudo-spectral I (60 Polynomials) | Pseudo-spectral II (40 polynomials) | AIM 100 Iterations |
|---|---|---|
| $-0.125000i$ | $-0.125000i$ | $-0.125000i$ |
| $-0.375602i$ | $-0.375602i$ | $-0.378659i$ |
| $-0.626877i$ | $-0.626877i$ | $-0.623931i$ |
| $-0.878946i$ | $-0.878948i$ | $-0.907374i$ |

# Conclusions and Perspectives

Investigated classical phenomena in multiple models of black hole binaries, among them

- Energy extraction via PP
- Quasinormal Modes
- Wave Scattering

# Conclusions and Perspectives

## Regarding the PP

- Energy extraction becomes increasingly effective in the presence of charged and rotating binaries.

- Devised an innovative technique that extends the analysis of energy extraction in a single black hole to arbitrary spacetimes, including numeric ones.

- Provided a proof-of-concept example featuring a superimposed Kerr binary, which confirms that the energy extraction efficiency is enhanced by the presence of a secondary object.

# Conclusions and Perspectives

## Regarding Quasinormal Modes

- A numerical package with broad applicability for computing quasinormal frequencies of black hole spacetimes has been developed.

- This package employs the recently developed Asymptotic Iteration Method and can easily handle multiple systems, that is, those whose perturbation evolutions can be written as second-order ODEs.

- We have revisited the perturbation problem in the Schwarzschild spacetime, comparing results with pseudospectral methods, WKB approximation, and Leaver's continued fraction method.

- We have computed new quasinormal frequencies for spin 5/2 perturbations, highlighting that these perturbations also possess purely imaginary frequencies.

# Conclusions and Perspectives

## Regarding wave scattering

- Created EinsteinToolkit Thorn, called FieldPerturbations, for the numerical evolution of a scalar field superimposed on a dynamically evolving metric.

- Demonstrated that the field profile displays a damped oscillatory phase following a highly nonlinear scattering, which bears similarities to the behavior observed when perturbing a single black hole.

- Distinct differences prohibit the direct fitting of a damped sine or cosine to the signal

- These results are preliminary, and more rigorous testing is pending.

# Conclusions and Perspectives

## Perspectives

- Study the Penrose process in dynamic spacetimes into fully dynamical simulations.

- Utilizing the EinsteinToolkit infrastructure to compute orbits as a background metric is evolved, or even using tables of a numerically evolved metric as input for our own code.

- Separate the PDEs that arise from analytical models of binary spacetimes by employing series approximations.

- Further explore the numerical simulation of the scalar field on the top of the GW150914 binary, searching for potential energy growth via superradiant scattering, analyzing the profile of the field to identify quasinormal frequencies, and investigating other spin perturbations. Consider backreaction.

# Conclusions and Perspectives

Thank You!